Dalton
Transactions

RSCPublishing

PAPER

View Article Online
View Journal | View Issue

Cite this: *Dalton Trans.*, 2013, **42**, 16185

Triple-stranded ferric helices: a π–π interaction-driven structural hierarchy of Fe_5, Fe_7, and Fe_{17} clusters†

Takuya Shiga, Mao Noguchi, Hiroki Sato, Takuto Matsumoto, Graham N. Newton and Hiroki Oshio*

Received 4th June 2013,
Accepted 5th September 2013

DOI: 10.1039/c3dt51480c

www.rsc.org/dalton

Three polypyridine ligand-supported multinuclear iron complexes, [Fe_5], [Fe_7] and [Fe_{17}], were synthesized and their physical properties were investigated. The complexes had triple-stranded helical structures with pseudo threefold symmetry, and were stabilized by varying degrees of intramolecular π–π stacking. The pentanuclear iron complex consisted of two Fe^{II} and three Fe^{III} ions, supported by three ligands, while the heptanuclear complex comprised four Fe^{II} centres, three Fe^{III} ions, and six ligands, and the heptadecanuclear complex contained seventeen Fe^{III} ions and nine ligands. Electrochemical studies revealed that the pentanuclear and heptanuclear iron complexes showed pseudo-reversible three- and five-step redox behaviours, respectively. Magnetic measurements conducted on the pentanuclear and heptanuclear complexes revealed that antiferromagnetic interactions were operative between neighbouring iron ions through the oxo- and pyrazole-bridges.

Introduction

Self-assembly of metal complexes is a useful approach for the construction of functional molecules and candidates for the next generation of molecule-based nano-scale electronic devices.[1] Complexes with regular arrays of metal ions, such as grids, rings, wheels, wires, helices and cages, have been prepared using appropriate ligands and have shown functionalities on the molecular level.[2] Planar multidentate ligands can be used to isolate grid-type molecules due to their rigidity and denticity, and Lehn *et al.* reported $[n \times n]$ grid complexes with polypyridine-type ligands,[3] while Thompson *et al.* used hydrazone-type ligands to prepare giant grids.[4] Complexes with wheel or ring motifs have usually been derived from bridging ligands with well-defined complementary coordination vectors.[5] Pecoraro *et al.* reported various metallacrown molecules supported by oxime ligands,[6] and a range of alkoxo-bridged wheel molecules were synthesized by Saalfrank *et al.*[7] In general, wheel and ring molecules include template ions or guest molecules at their centre as a means of stabilizing their molecular shape. Thus, the molecular design of such complexes must consider both the bridging ligands and template molecules. For example, Dunbar *et al.* investigated the anionic template-controlled selective synthesis of square-type and pentanuclear ring complexes.[5] Molecular wires supported by polypyridylamine ligands were reported by Peng *et al.*[8] Planar multidentate ligands can integrate metal ions in a linear fashion; however, there are also numerous examples where such ligands have led to the isolation of helical structures. Lehn *et al.* have reported the formation of helical molecules using a pyrimidine-hydrazone ligand,[9] and Kawata *et al.* reported magnetically frustrated helicates with the pyridyl-pyrazole-type ligand, 3,5-bis(2-pyridyl)pyrazolate.[10] Complexes with cage-type architectures have been synthesized by Fujita *et al.*, Raymond *et al.*, Ward *et al.*, and Zaworotko *et al.*, amongst others, and their nano-space science has been investigated.[11] These cage compounds were formed utilizing the coordination chemistry of transition metal ions and rigid heterocyclic ligands. The establishment of rational syntheses of these cluster compounds with regular metal ion arrays is an important goal, due to their potential to act as molecular-based functional materials. The magnetic properties of polynuclear complexes continue to attract much attention due to their structure-specific phenomena, such as quantum magnetism[12] and electron-transfer-coupled spin transition (ETCST).[13] Their multi-redox behaviour is another facet of their physical characteristics that may have applications in future molecular-switching materials.[14] The development of novel high-nuclearity metal clusters and subsequent elucidation of their physical properties is thus a vital goal in the search for new functional materials.

Multidentate ligands are useful tools for the synthesis of function-programmed polynuclear complexes,[15] and the

---

Department of Chemistry, Graduate School of Pure and Applied Sciences, University of Tsukuba, Tennodai 1-1-1, Tsukuba 305-8571, Japan. E-mail: oshio@chem.tsukuba.ac.jp; Fax: +81-29-853-4238; Tel: +81-29-853-4238

†Electronic supplementary information (ESI) available: Mössbauer data of complex **2**. CCDC 942566–942568. For ESI and crystallographic data in CIF or other electronic format see DOI: 10.1039/c3dt51480c

development of new systems is dependent on full investigation of a ligand's complexation behaviour with a range of metal ions. We previously reported the wheel-like heptanuclear manganese single-molecule magnet, $[Mn^{II}_3Mn^{III}_4(5\text{-}NO_2\text{-hbide})_6]\cdot5C_2H_4Cl_2$ ($H_3(5\text{-}NO_2\text{-hbide})$ = *N*-(2-hydroxy-5-nitrobenzyl)iminodiethanol), in which the alkoxo groups of the ligand stabilize the Mn_7O_{12} core structure.[16] Moreover, a giant oxo-bridged $[Mn_{12}Cu_8]$ cluster was obtained by using a Schiff-base/alkoxo ligand.[17] In general, alkoxo-type ligands can effectively interact with metal ions; however, the products can be unpredictable. On the other hand, a ligand with well-defined coordination vectors allows the synthesis of structurally- (and thus functionally-) designable clusters. Polycyanide complexes are a good example of such building blocks. Recently we reported a cyanide bridged tetranuclear complex, $[Co_2Fe_2]$, which showed step-wise ETCST behaviour.[18] In another example, a ferromagnetically coupled $[Ni_6Fe_4]$ cyanide-bridged cluster was obtained using chiral ligands.[19] Such complexes can display a range of functionalities, depending on their shape and metal ion composition. However, their feasible range of properties is limited due to the magnetic and electronic interactions through the CN bridges. We are currently attempting to develop a family of new cluster molecules supported by a polypyridine-type multidentate ligand.[20,21] A $[Co_9]$ grid-type single-molecule magnet was synthesized by the reaction of H_2L (H_2L = 2,6-bis[5-(2-pyridinyl)-1*H*-pyrazole-3-yl]-pyridine) with $Co(BF_4)_2\cdot6H_2O$,[20] showing the polypyridyl-type ligand, H_2L, to have the potential to form pyrazole-bridged polynuclear complexes with specific physical properties. Subsequently, the complexation dynamics of H_2L with cobalt and iron ions were investigated using time-resolved cryo-spray ESI-MS measurements.[21] In order to further develop our research in this area, this paper deals with the complexation behaviour of H_2L with iron ions under a range of reaction conditions. Three helical iron complexes are herein introduced, and their magnetic properties and electrochemical features are presented.

Experimental section

Materials and physical measurements

All chemicals used during the syntheses were reagent grade. The multidentate ligand, H_2L, was prepared following a previously reported method.[20]

Synthesis of $[Fe^{II}_2Fe^{III}_3(L)_3(\mu_3\text{-}O)(\mu_2\text{-}OMe)(OAc)_2]Cl_2\cdot MeOH\cdot 7.5H_2O$ (1·MeOH·7.5H$_2$O). To a pale yellow solution of H_2L (60.0 mg, 0.16 mmol) and triethylamine (44 μL, 0.32 mmol) in methanol (5 mL) a solution of $FeCl_2\cdot4H_2O$ (63.5 mg, 0.32 mmol) and $La(OAc)_3\cdot nH_2O$ (50.5 mg, 0.16 mmol) in methanol (10 mL) was added and the resulting mixture was stirred and heated for 10 minutes. The reaction mixture turned from pale yellow to dark reddish-brown and was then filtered and left at room temperature to crystallize by slow evaporation. Rod-like reddish-brown crystals, suitable for X-ray structural analysis, of $[Fe^{II}_2Fe^{III}_3(L)_3(\mu_3\text{-}O)(\mu_2\text{-}OMe)(OAc)_2]Cl_2\cdot6MeOH\cdot2H_2O$ (**1·6MeOH·2H$_2$O**) were obtained. The crystals were collected by suction and air-dried, affording $[Fe^{II}_2Fe^{III}_3(L)_3(\mu_3\text{-}O)(\mu_2\text{-}OMe)(OAc)_2]Cl_2\cdot MeOH\cdot7.5H_2O$ (**1·MeOH·7.5H$_2$O**). Elemental analysis (%) calcd for $C_{69}H_{67}N_{21}Cl_2O_{14.5}Fe_5$: C 46.75, H 3.81, N 16.59; found: C 46.62, H 3.51, N 16.29. IR (KBr, cm^{-1}): 1438.8, 1463.9, 1544.9, 1568.0, 1604.7.

Synthesis of $[Fe^{II}_4Fe^{III}_3(HL)(H_2L)_5(\mu_2\text{-}OH)_6(OH)_6](BF_4)_4\cdot2MeOH\cdot6H_2O$ (2·2MeOH·6H$_2$O). To a solution of H_2L (21.9 mg, 0.06 mmol) and triethylamine (16.5 μL, 0.12 mmol) in methanol (13 mL) a solution of $Fe(BF_4)_2\cdot6H_2O$ (67.5 mg, 0.20 mmol) in methanol (15 mL) was added. The reaction mixture was stirred for several minutes and then filtered and left at room temperature to evaporate. After a few days, diffraction-suitable rod-like reddish-brown crystals of $[Fe^{II}_4Fe^{III}_3(HL)(H_2L)_5(\mu_2\text{-}OH)_6(OH)_6](BF_4)_4\cdot8.5MeOH\cdot8H_2O$ (**2·8.5MeOH·8H$_2$O**) were obtained. The crystals were collected by suction and air-dried, affording $[Fe^{II}_4Fe^{III}_3(HL)(H_2L)_5(\mu_2\text{-}OH)_6(OH)_6](BF_4)_4\cdot2MeOH\cdot6H_2O$ (**2·2MeOH·6H$_2$O**). Elemental analysis (%) calcd for $C_{128}H_{126}N_{42}B_4F_{16}Fe_7O_{22}$: C 45.99, H 3.80, N 17.60; found: C 45.95, H 3.13, N 17.37. IR (KBr, cm^{-1}): 783.0, 1437.8, 1472.5, 1569.9, 1607.6.

Synthesis of $[Fe^{III}_{17}(L)_9(\mu_3\text{-}O)_{13}(\mu_3\text{-}OH)](PF_6)_6\cdot8CH_3CN\cdot2H_2O$ (3·8CH$_3$CN·2H$_2$O). Currently, compound **3**‡ can only be prepared in a mixture with visually indistinguishable crystals of a pentanuclear triazole bridged $[Fe_5]$ cluster, $[Fe_5(L)_3(\mu_3\text{-}O)(trz)_3]Cl_5$.[22] At this stage, our inability to obtain a sufficient quantity of pure sample means that the physical properties of **3** cannot be investigated, and herein only the structure is presented. We are now attempting to use ESI-MS techniques to improve the synthetic method. The synthesis adopted herein is reported in the ESI.†

X-ray crystallography

The crystals were mounted on glass capillaries, and data were collected at −173 °C (a Bruker SMART APEX diffractometer coupled with a CCD area detector with graphite monochromated MoKα (λ = 0.71073 Å) radiation). The structure was solved using direct methods and expanded using Fourier techniques within the SHELXTL program. Empirical absorption

---

‡Crystallographic data for **1**: $(C_{68}H_{48}Fe_5N_{21}O_6)Cl_2\cdot6CH_3OH\cdot2H_2O$, M_r = 1833.71, monoclinic $C2/c$, a = 17.328(6) Å, b = 21.331(7) Å, c = 22.382(8) Å, β = 90.680(6)°, V = 8178(5) Å^3, Z = 4, T = 100 K. A total of 16 490 reflections were collected (4.24° < 2θ < 46.7°), of which 5833 unique reflections (R_{int} = 0.0686) were measured. R_1 = 0.0555, wR_2 = 0.1290 ($I > 2\sigma(I)$).

2: $(C_{126}H_{101}Fe_7N_{42}O_{12})(BF_4)_4\cdot8.5CH_3OH\cdot8H_2O$, M_r = 3533.03, orthorhombic $P2_12_12$, a = 18.690(2) Å, b = 26.157(3) Å, c = 32.885(4) Å, V = 16 077(3) Å^3, Z = 4, T = 100 K. A total of 73 648 reflections were collected (1.24° < 2θ < 46.56°), of which 23 122 unique reflections (R_{int} = 0.0415) were measured. R_1 = 0.0658, wR_2 = 0.1836 ($I > 2\sigma(I)$).

3: $(C_{189}H_{117}Fe_{17}N_{63}O_{14})(PF_6)_6\cdot8CH_3CN\cdot2H_2O$, M_r = 5678.19, trigonal $R32$, a = 28.011(2) Å, b = 28.011(2) Å, c = 25.438(3) Å, V = 17 285(3) Å^3, Z = 3, T = 100 K. A total of 23 428 reflections were collected (4.64° < 2θ < 46.56°), of which 5535 unique reflections (R_{int} = 0.2171) were measured. R_1 = 0.0877, wR_2 = 0.2034 ($I > 2\sigma(I)$). Disordered solvent molecules in the crystal voids have been removed from calculations by the SQUEEZE program.[35]

Cif files for **1**, **2** and **3** are available from CCDC with deposition numbers CCDC 942566–942568.

corrections were carried out using SADABS. In the structure analyses, non-hydrogen atoms were refined with anisotropic thermal parameters. Hydrogen atoms were included in calculated positions and refined with isotropic thermal parameters riding on those of the parent atom.

Physical measurements

Magnetic susceptibility data were collected using a Quantum Design MPMS-5S SQUID magnetometer. Magnetic data were corrected for the diamagnetic contribution of the sample holder, and the diamagnetism of the samples was accounted for using Pascal's constants. Analyses of magnetic data were performed using the MAGPACK program.[23] Mössbauer experiments were carried out using a ^{57}Co/Rh source in a constant-acceleration transmission spectrometer (Topologic Systems) equipped with an Iwatani HE05/CW404 cryostat. The spectra were recorded at 20 K and 300 K for complex **2**. The spectrometer was calibrated using standard α-Fe foil. Electrochemical measurements were carried out using a BAS 620A electrochemical analyser. Cyclic voltammetry and differential pulse voltammetry measurements were carried out in a standard one-compartment cell under N_2 at 20 °C equipped with a platinum-wire counter electrode, a saturated calomel electrode (SCE) as the reference electrode, and a glassy carbon (GC) working electrode.

Results and discussion

Syntheses

The heptadentate polypyridine ligand, 2,6-bis[5-(2-pyridinyl)-1*H*-pyrazole-3-yl]pyridine (Scheme 1), was prepared from the reaction of 2,6-bis[3-(2-pyridine)-1,3-dioxopro-pyl]pyridine with hydrazine monohydrate, as described previously.[20] All iron complexes were synthesized under aerobic conditions; if the syntheses were performed under an inert atmosphere, a ring-type molecule was obtained, which will be described in a future communication. In the synthesis of **1**, the use of $La(OAc)_3$ as an acetate source was found to maximize the yield, possibly resulting from the perturbation of the reaction dynamics brought about by the Lewis acidity of the lanthanum ions. Triazole was used in the synthesis of **3**, due to its weak basicity and potential to function as a bridging ligand, aiding the formation of larger polynuclear clusters.

Crystal structure of 1

The molecular structure of the pentanuclear complex, $[Fe^{II}_2Fe^{III}_3(L)_3(\mu_3\text{-}O)(\mu_2\text{-}OMe)(OAc)_2]Cl_2\cdot 6MeOH\cdot 2H_2O$ (**1·6MeOH·2H₂O**), is presented in Fig. 1. **1** crystallized in the monoclinic space group *C*2/*c*. In **1**, three doubly-deprotonated ligands coordinate five iron ions in a spiral manner forming a pentanuclear helical complex. The asymmetric unit contains half of one $[Fe_5(L)_3(\mu_3\text{-}O)(\mu_2\text{-}OMe)(OAc)_2]$ cluster, one Cl^- anion, three methanol moieties and one water molecule. The molecule has a two-fold axis passing through the Fe1, O1, O2, N4, C11 and C33 atoms. All iron ions have octahedral coordination environments, but there are two distinct types of iron ions, one located in the central triangular core and the other isolated at the tip of the helix. The Fe1 ion, of the central Fe_3O core, is co-ordinated by a N_3O_3 donor set consisting of the tridentate site of one ligand, the oxygen atoms of two bridging AcO^- anions and the central μ_3-oxo ligand. The Fe2 ion, which is also located in the Fe_3O triangular core, has a N_3O_3 donor set comprised of one tridentate ligand, one acetate oxygen atom, one methoxide oxygen atom and the central μ_3-oxo ion. Fe3 exists in an N_6 donor set, coordinated by the terminal bidentate sites of three L groups.

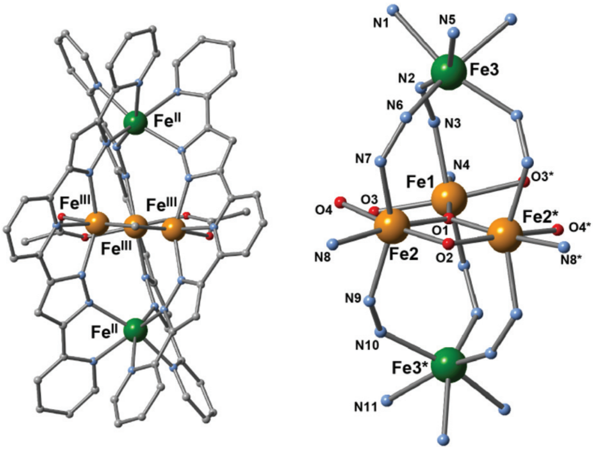

Fig. 1 Molecular structures of the cationic moiety of **1** (left) and the core structure of **1** (right). Hydrogen atoms are omitted for clarity.

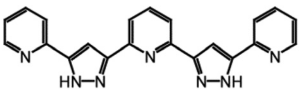

Scheme 1 Heptadentate polypyridine ligand H_2L.

The iron ions have average coordination bond lengths of 2.051, 2.048 and 2.207 Å for Fe1, Fe2 and Fe3 respectively. Bond valence sum (BVS) calculations and charge balance suggest that the Fe1 and Fe2 ions are trivalent and that the Fe3 ions are divalent.[24] The Fe_3O core is almost planar, but the contrasting intermetallic separations of 3.409 and 3.009 Å between the acetate-bridged (Fe1···Fe2) and the methoxy-bridged (Fe2···Fe2*) ions respectively render the core an isosceles triangle.

This structure is similar to the $[M_5]$ complexes reported by Kawata *et al.*[10] However, **1** differs from the previously reported $[M_5]$ complexes in its symmetry: the $[M_5]$ complexes have equilateral triangular cores. Complex **1** has a similar core structure to the previously reported heptanuclear iron complex, which derived from the Hbpt ligand.[25]

Crystal structure of 2

The heptanuclear iron complex, $[Fe^{II}_4Fe^{III}_3(HL)(H_2L)_5(\mu_2\text{-}OH)_6(OH)_6](BF_4)_4\cdot 8.5MeOH\cdot 8H_2O$ (**2·8.5MeOH·8H₂O**), is represented in Fig. 2. **2** crystallized in the orthorhombic space group

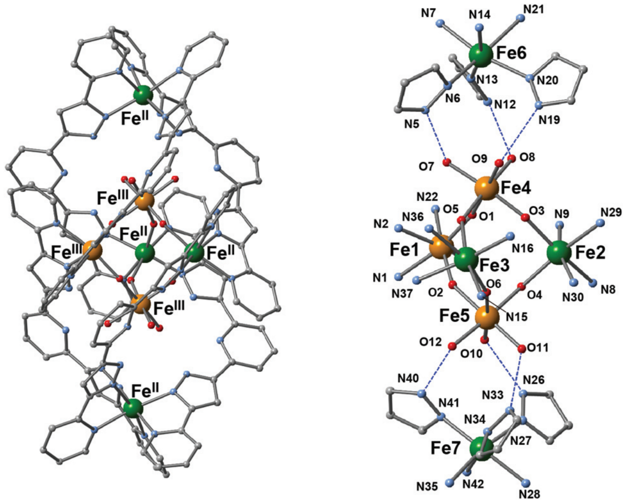

Fig. 2 Molecular structure of the cationic moiety of **2** (left), and the core of **2** with hydrogen bonding interactions (right). Hydrogen atoms are omitted for clarity.

$P2_12_12$, and was structurally characterised to consist of six ligands, one of which was suggested to be singly-deprotonated based on charge balance considerations, and seven iron ions with twelve hydroxide anions. The iron ions can be categorised into a central pentanuclear unit and two terminal mononuclear moieties, but in terms of coordination environment, there are three kinds of iron ion, corresponding to the ions in the central (Fe1, Fe2, and Fe3), middle (Fe4 and Fe5), and terminal (Fe6 and Fe7) sites.

The iron ions in the central sites have N_4O_2 donor sets composed of four nitrogen atoms of two bidentate ligand groups and two bridging hydroxide anions, while the middle iron ions have O_6 donor sets, coordinated by three μ_2-hydroxo anions and three capping hydroxo ligands as determined by BVS.[26a] The terminal iron ions have N_6 donor environments, coordinated by the terminal bidentate sites of three ligands. The BVS calculations imply that two of the central and both terminal iron ions are divalent and that the remaining central (Fe1) and middle iron ions are trivalent.[26b] In this molecule, the ligand pyrazole moieties are protonated and form hydrogen-bonded interactions to the hydroxo groups bound to the middle iron ions. In total, one complex molecule contains six hydrogen bonds. These intramolecular hydrogen bonds, coupled with π–π stacking interactions between neighbouring ligands, stabilize the heptanuclear helical structure. It is interesting to note that the structure of **2** very closely resembles that of a $[Fe^{III}_2Co^{II}_5]$ complex, previously reported with the same ligand, that was found to be a stable intermediate in the synthesis of a $[Fe^{II}_4Fe^{III}Co^{II}_4]$ grid. Future work will investigate the solution-state assembly of these related homometallic clusters.

Crystal structure of 3

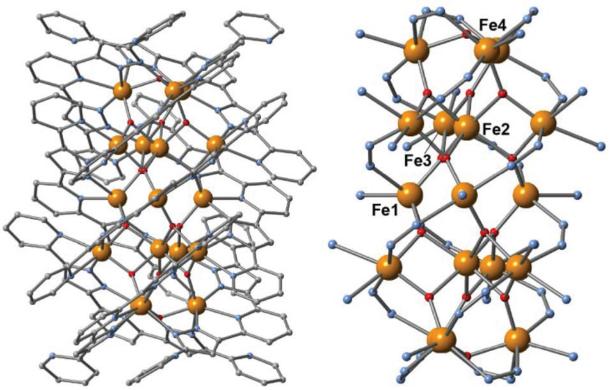

Fig. 3 Molecular structure of the cationic moiety of **3** (left), and the core structure (right). Hydrogen atoms are omitted for clarity.

Crystal structure diagrams of the giant heptadecanuclear iron complex, $[Fe^{III}_{17}(L)_9(\mu_3\text{-}O)(\mu_3\text{-}OH)](PF_6)_6\cdot 2H_2O\cdot 8CH_3CN$ ($\mathbf{3}\cdot 2H_2O\cdot 8CH_3CN$), are shown in Fig. 3. **3** crystallized in the trigonal space group *R*32. Nine doubly-deprotonated ligands coordinate seventeen iron ions, forming a triple stranded helical structure with a strict threefold rotation axis. All iron ions are trivalent, as confirmed by charge balance and BVS calculations.[27] The core (Fig. 3, right) can be considered as five parallel layers of three types in a CBABC arrangement. Layer A is an iron triangle (Fe1) linked by O–Fe2–O bridges; Layer B is a triangular tetranuclear unit (Fe2 and Fe3) with a 'Mitsubishi' logo-like shape; and Layer C is a trinuclear triangular unit (Fe4). The threefold axis passes through the O3–Fe2–Fe2$^\#$–O3$^\#$ centres (symmetry operation #: +*y*, +*x*, −*z*). Each layer is linked to its neighbours by pyrazole and oxo bridges (Fig. 4).

All iron ions have distorted octahedral coordination environments with the exception of the Fe1 ion, which has a five-coordinate trigonal bipyramidal geometry. The Fe1 ions of Layer A are coordinated by three ligand nitrogen atoms and two bridging oxo ions. The Fe2 ions are located at the centre of the Layer B triangular unit and are coordinated by six bridging oxo ions. The Fe3 ions in Layer B are coordinated by four nitrogen atoms from the bidentate sites of two ligands and two bridging oxo ions. The Fe4 ions in Layer C are bound by the

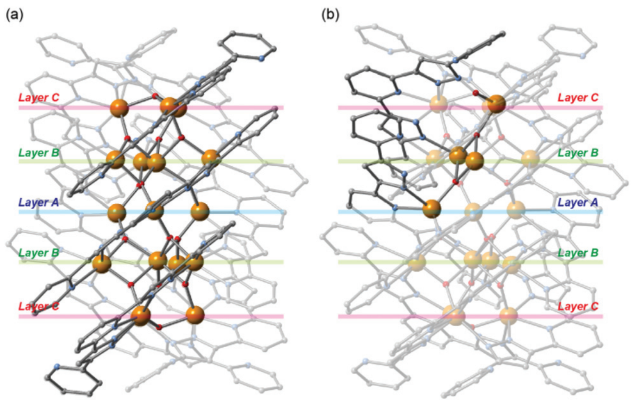

Fig. 4 Molecular structure of **3** with three layers (see text). The triple π stacking ligands (left) and asymmetric units (right) are highlighted.

four nitrogen atoms of two bidentate ligand binding sites and two bridging oxo (or one oxo and one hydroxo ion). There are double π–π stacking interactions between three neighbouring ligands, and additional π–π interactions between the terminal pyridine rings of the top and bottom of the stacked ligands and the central pyridine rings of the neighboring stacked ligands, causing one pyridyl group to twist from the ligand plane. This giant cluster arrangement of iron ions is very unusual, as most large iron clusters have ring or planar wheel-based structures, in which oxo ions are located on the surface of the molecules (Fig. 5).

Exceptions to this were the [Fe_{17}] cluster reported by Brechin, Collison and Heath,[28] and the [Fe_{19}] complex reported by Brechin and McInnes.[29] Ferritin, a well-known protein with a large structure (~12 nm), can store huge numbers (~4500) of iron atoms as ferric oxide.[30] In the present molecule, the oxo ions exist inside the cluster and its surface is covered by polypyridine ligands. This similarity will open the possibility of the development of artificial ferritin.

All three complexes have helical structures and there is a corresponding hierarchy of π–π stacking interactions. **1** exhibits no π–π stacking, whereas **2** shows π–π interactions between dimerized ligands. In contrast, **3** displays double π–π stacking interactions between trimers of ligands (Fig. 6).

Magnetic properties

The magnetic susceptibilities for **1** and **2** were measured on powdered polycrystalline samples under a constant magnetic field of 0.05 T, in the 1.8–300 K range. The results for **1** and **2** are represented in Fig. 7 and 8 respectively as $\chi_m T$ *versus* T plots.

In **1**, the $\chi_m T$ value at 300 K was 10.75 emu mol^{-1} K, much smaller than the spin-only value of $\chi_m T$ = 19.125 emu mol^{-1} K expected for the sum of the magnetically isolated spins of two Fe^{II} (high-spin) and three Fe^{III} (high-spin) ions with g = 2.00. As the temperature was lowered, the $\chi_m T$ values decreased, reaching a minimum value of 2.61 emu mol^{-1} K at 1.8 K, indicative of the existence of antiferromagnetic interactions between the iron ions. Considering the specific bridges between the metal ions, a pentanuclear spin model for magnetic analysis can be assumed, as shown in Fig. 7 (inset). The spin Hamiltonian of this system has the form given in eqn (1):

$$\begin{aligned}\hat{H} = & -2J_1(\hat{S}_2\cdot\hat{S}_3) - 2J_2(\hat{S}_1\cdot\hat{S}_2 + \hat{S}_1\cdot\hat{S}_3) \\ & -2J_3(\hat{S}_1\cdot\hat{S}_4 + \hat{S}_2\cdot\hat{S}_4 + \hat{S}_3\cdot\hat{S}_4 + \hat{S}_1\cdot\hat{S}_5 + \hat{S}_2\cdot\hat{S}_5 + \hat{S}_3\cdot\hat{S}_5)\end{aligned} \tag{1}$$

Fitting of the experimental data gave $g_{av.}$ = 2.02, J_1 = −150.0 K, J_2 = −20.0 K, and J_3 = −0.4 K, suggesting the

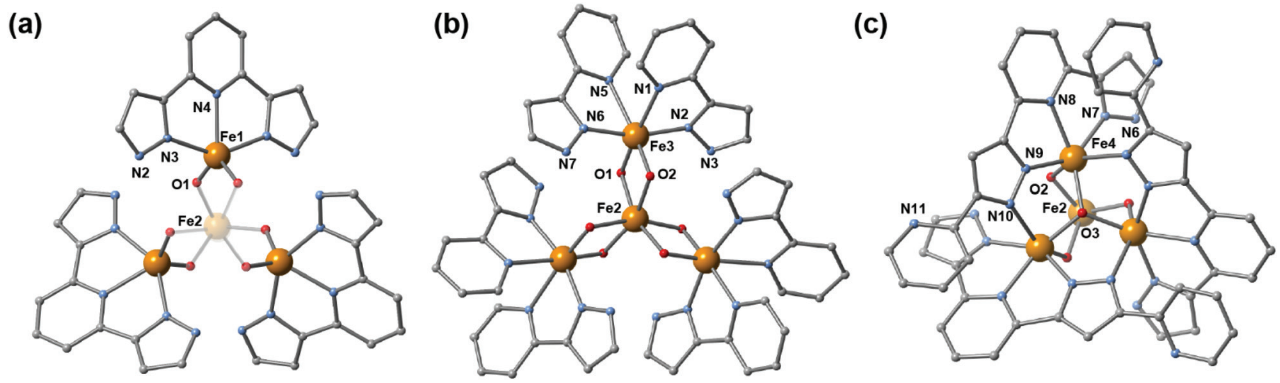

Fig. 5 Partial structure of complex **3**. (a) Layer A, (b) Layer B, and (c) Layer C.

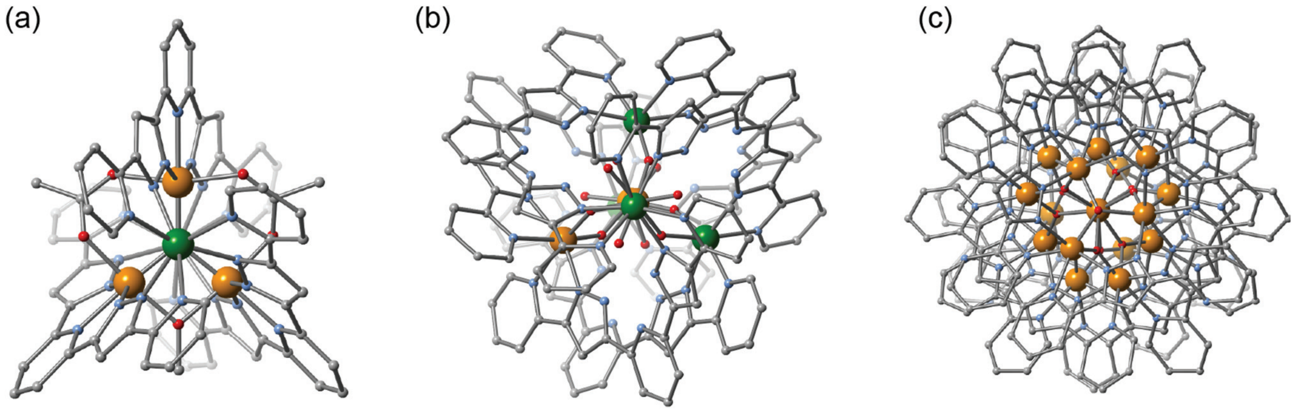

Fig. 6 Top views of three complexes. Left: [Fe_5] complex (**1**), middle: [Fe_7] complex (**2**), right: [Fe_{17}] complex (**3**).

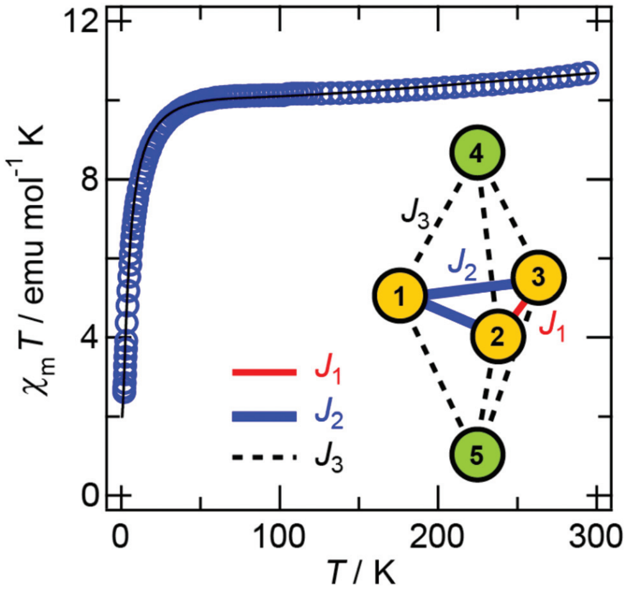

Fig. 7 $\chi_m T$ *versus* *T* plots of **1**. The solid line is the fit of the experimental data (see text). The schematic drawing in the inset is the spin model (yellow and green circles represent Fe^{III} and Fe^{II}, respectively).

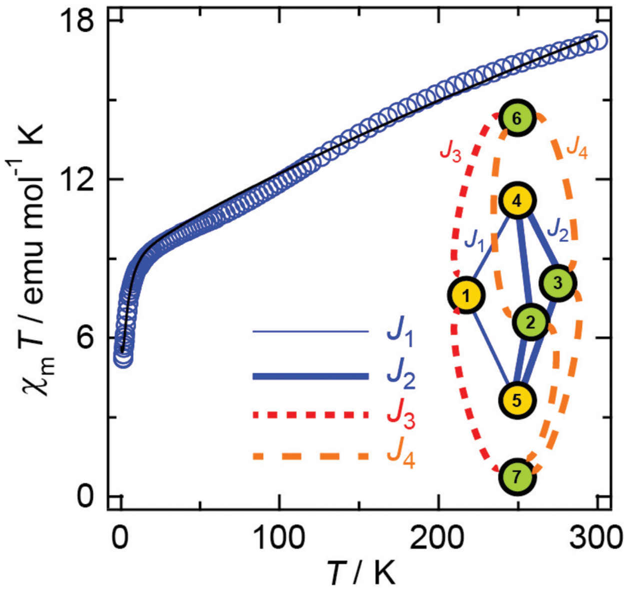

Fig. 8 $\chi_m T$ *versus* *T* plots of **2**. The solid line is the fit of the experimental data (see text). The schematic drawing in the inset is the spin model (yellow and green circles represent Fe^{III} and Fe^{II}, respectively).

existence of strong antiferromagnetic interactions between the three Fe^{III} ions in the central trinuclear core through the μ_3-O^{2-} bridge, which mediates short metal–metal separations and obtuse bridging angles.[31] The magnetic path between the central trinuclear unit and the terminal Fe^{II} ions is mediated by the pyrazole units, and is likely to be relatively weak, due to the two atom bridges.[32] Moreover, magnetic interactions through pyrazolate bridges depend on the angles between the magnetic orbitals of the metal ions and the pyrazole ring.[33] In **1**, the magnetic orbitals of the terminal Fe^{II} ions and the pyrazole ring are non-coplanar, and the resulting antiferromagnetic interactions are very weak.

For **2**, the $\chi_m T$ value of 17.25 emu mol^{-1} K at 300 K is smaller than the expected value (25.125 emu mol^{-1} K) for the sum of the uncorrelated spins of four Fe^{II} (high-spin) and three Fe^{III} (high-spin) ions. As the temperature was decreased, the $\chi_m T$ value decreased, reaching a value of 5.21 emu mol^{-1} K at 1.8 K, suggesting that antiferromagnetic interactions were operative between the iron ions. The magnetic data were fitted to the isotropic exchange Hamiltonian given in eqn (2):

$$\hat{H} = -2J_1(\hat{S}_1\cdot\hat{S}_4 + \hat{S}_1\cdot\hat{S}_5) - 2J_2(\hat{S}_2\cdot\hat{S}_4 + \hat{S}_2\cdot\hat{S}_5 + \hat{S}_3\cdot\hat{S}_4 + \hat{S}_3\cdot\hat{S}_5) \\ -2J_3(\hat{S}_1\cdot\hat{S}_6 + \hat{S}_1\cdot\hat{S}_7) - 2J_4(\hat{S}_2\cdot\hat{S}_6 + \hat{S}_2\cdot\hat{S}_7 + \hat{S}_3\cdot\hat{S}_6 + \hat{S}_3\cdot\hat{S}_7) \tag{2}$$

Fitting of the experimental data gave $g_{av.}$ = 2.30, J_1 = −10.0 K, J_2 = −40.0 K, J_3 = −0.15 K, and J_4 = −0.20 K. The antiferromagnetic interactions between Fe^{II} and Fe^{III} ions in the central pentanuclear core were strong due to the μ_2-hydroxo bridging, and resulted in an overall residual coupled spin of *S* = 3/2 in the heptanuclear moiety. In the magnetic analysis, four separate magnetic coupling pathways were considered, according to the bridging groups and the Fe–O–Fe bridging angles. The two terminal *S* = 2 iron(II) centres are very weakly antiferromagnetically coupled to the pentanuclear core. With this in mind, the magnetic properties at low temperature can be considered as the combination of three paramagnetic units, with *S* = 2 + 3/2 + 2, for which the spin only value is 7.875 emu mol^{-1} K (*g* = 2.00). The $\chi_m T$ value of **2** at 10 K was 8.54 emu mol^{-1} K, which agrees with the model owing to the large *g* values expected for high-spin Fe^{II} ions. Mössbauer data excluded the possibility that the decreased susceptibility derived from iron spin-crossover phenomena due to the temperature-independence of the signal intensities (Fig. S1†). The very low yield in which **3** was obtained prevented the collection of reliable magnetic data.

Electrochemical properties

The electrochemical properties of **1** and **2** were investigated in acetonitrile, and the cyclic voltammogram of **1** is shown in Fig. 9. **1** shows three quasi-reversible redox waves at +0.85, +0.70, and −0.28 V (*versus* SCE). Considering the redox potential of $[Fe(bpy)_3]$ (+0.66 V *versus* Fc/Fc$^+$; approx. +1.06 V *versus* SCE),[34] the two oxidation processes at +0.85 and +0.70 V were assigned as the Fe^{II}/Fe^{III} redox waves of the two terminal iron ions. The reduction process at −0.28 V corresponded to the Fe^{III}/Fe^{II} redox of the iron ions on the central triangular unit.

The cyclic voltammogram of **2** is shown in Fig. 10, and exhibits five quasi-reversible redox processes. The rest potential was located at +0.38 V and the voltammogram suggested the occurrence of two reduction and three oxidation processes. In its initial state, **2** has three Fe^{III} and four Fe^{II} ions. Therefore, the two reduction peaks were assigned as the reduction processes of two of the trivalent ions, while the three oxidation peaks corresponded to the oxidation of the

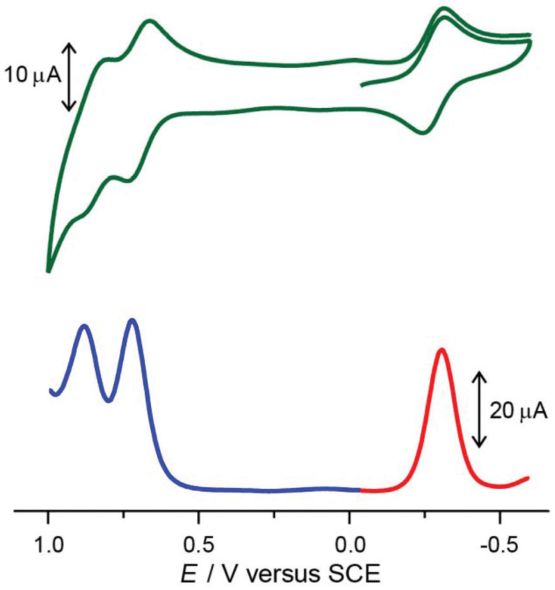

Fig. 9 Cyclic voltammogram of **1** (top) and dpv (bottom).

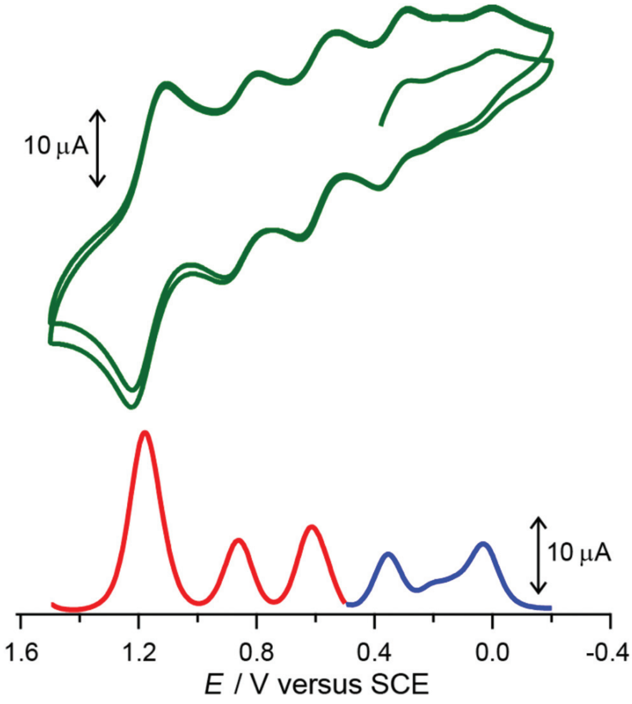

Fig. 10 Cyclic voltammogram of **2** (top) and dpv (bottom).

iron ions occupying the central and terminal sites. The oxidation peaks at +0.60 and +0.86 V are very close to the oxidation potentials of the iron ions in the terminal sites of **1**, so they were assigned as the oxidation peaks of the corresponding terminal iron ions in **2**. Considering the structure of **2**, the oxidation peak at 1.17 V was assigned as the redox process of the two divalent iron ions in the central coordination sites.

Complexes **1** and **2** show multi-stable redox behaviour with reasonable separation of the different charge states, resulting from intramolecular electronic cooperativity. These iron cluster systems and their related compounds therefore have potential of being used as electron-sink-type functional moieties in future molecular devices.

Conclusions

Three iron complexes were synthesized using the heptadentate polypyridine ligand, H_2L (= 2,6-bis[5-(2-pyridinyl)-1*H*-pyrazole-3-yl]pyridine). All complexes had triple-stranded helical structures with pseudo threefold symmetry. The pentanuclear iron complex $[Fe_5]$ (**1**) consisted of two Fe^{II} and three Fe^{III} ions with three ligands, the heptanuclear iron complex $[Fe_7]$ (**2**) was comprised of four Fe^{II} and three Fe^{III} ions with six ligands and the heptadecanuclear iron complex $[Fe_{17}]$ (**3**) was composed of seventeen Fe^{III} ions and nine ligands. The differences in the hierarchical π–π stacking exhibited by the three complexes leads to the diversity of cluster size. Magnetic measurements conducted on the pentanuclear and heptanuclear complexes revealed that antiferromagnetic interactions were operative between neighbouring iron ions, mediated by oxo- and pyrazole-bridges. Electrochemical studies revealed the pentanuclear and heptanuclear iron complex to show pseudo-reversible three and five-step redox behaviours, respectively.

Acknowledgements

The authors gratefully acknowledge a Grant-in-Aid from the Japanese Ministry of Education, Culture, Sports, Science and Technology (MEXT) (scientific research within the framework of the Priority Area *Coordination Programming*, area 2107).

Notes and references

1 Molecular electronics: (*a*) J. E. Green, J. W. Choi, A. Boukai, Y. Bunimovich, E. Johnston-Halperin, E. DeIonno, Y. Luo, B. A. Sheriff, K. Xu, Y. S. Shin, H.-R. Tseng, J. F. Stoddart and J. R. Heath, *Nature*, 2007, **445**, 414; (*b*) E. R. Kay, D. A. Leigh and F. Zerbetto, *Angew. Chem., Int. Ed.*, 2007, **46**, 72; (*c*) C. S. Lent, *Science*, 2000, **288**, 1597; (*d*) O. Sato, J. Tao and Y.-Z. Zhang, *Angew. Chem., Int. Ed.*, 2007, **46**, 2152; (*e*) G. A. Timco, S. Carretta, F. Troiani, F. Tuna, R. J. Pritchard, C. A. Muryn, E. J. L. McInnes, A. Ghirri, A. Candini, P. Santini, G. Amoretti, M. Affronte and R. E. P. Winpenny, *Nat. Nanotechnol.*, 2009, **4**, 173.

2 Regular metal array, reviews: (*a*) M. Ruben, J. Rojo, F. J. Romero-Salguero, L. H. Uppadine and J.-M. Lehn, *Angew. Chem., Int. Ed.*, 2004, **43**, 3644; (*b*) L. N. Dawe, K. V. Shuvaev and L. K. Thompson, *Chem. Soc. Rev.*, 2009, **38**, 2334; (*c*) G. A. Timco, T. B. Faust, F. Tuna and R. E. P. Winpenny, *Chem. Soc. Rev.*, 2011, **40**, 3067;

(*d*) R. W. Saalfrank, H. Maid and A. Scheurer, *Angew. Chem., Int. Ed.*, 2008, **47**, 8794; (*e*) J. J. Bodwin, A. D. Cutland, R. Malkani and V. L. Pecoraro, *Coord. Chem. Rev.*, 2001, **216–217**, 489; (*f*) M. Affronte, S. Carretta, G. A. Timco and R. E. P. Winpenny, *Chem. Commun.*, 2007, 1789.

3 Lehn's grid: (*a*) A. R. Stefankiewicz, G. Rogez, J. Harrowfield, A. N. Sobolev, A. Madalan, J. Huuskonen, K. Rissanen and J.-M. Lehn, *Dalton Trans.*, 2012, **41**, 13848; (*b*) M. Ruben, E. Breuning, J.-M. Lehn, V. Ksenofontov, F. Renz, P. Gütlich and G. Vaughan, *Chem.–Eur. J.*, 2003, **9**, 4422; (*c*) J. R. Nitschke and J.-M. Lehn, *Proc. Natl. Acad. Sci. U. S. A.*, 2003, **100**, 11970; (*d*) M. Barboiu, G. Vaughan, R. Graff and J.-M. Lehn, *J. Am. Chem. Soc.*, 2003, **125**, 10257; (*e*) L. H. Uppadine, J.-P. Gisselbrecht, N. Kyritsakas, K. Nattinen, K. Rissanen and J.-M. Lehn, *Chem.–Eur. J.*, 2005, **11**, 2549; (*f*) A. R. Stefankiewicz, J. Harrowfield, A. Madalan, K. Rissanen, A. N. Sobolev and J.-M. Lehn, *Dalton Trans.*, 2011, **40**, 12320; (*g*) N. Parizel, J. Ramírez, C. Burg, S. Choua, M. Bernard, S. Gambarelli, V. Maurel, L. Brelot, J.-M. Lehn, P. Tureky and A.-M. Stadler, *Chem. Commun.*, 2011, **47**, 10951.

4 Thompson's grid: (*a*) M. U. Anwar, L. K. Thompson, L. N. Dawe, F. Habibb and M. Murugesu, *Chem. Commun.*, 2012, **48**, 4576; (*b*) M. U. Anwar, K. V. Shuvaev, L. N. Dawe and L. K. Thompson, *Inorg. Chem.*, 2011, **50**, 12141.

5 Wheel and rings: (*a*) G. L. Abbati, A. Cornia, A. C. Fabretti, W. Malavasi, L. Schenetti, A. Caneschi and D. Gatteschi, *Inorg. Chem.*, 1997, **36**, 6443; (*b*) A. Cornia, M. Affronte, A. G. M. Jansen, G. L. Abbati and D. Gatteschi, *Angew. Chem., Int. Ed.*, 1999, **38**, 2264; (*c*) C. S. Campos-Fernández, R. Clérac and K. R. Dunbar, *Angew. Chem., Int. Ed.*, 1999, **38**, 3477; (*d*) C. S. Campos-Fernández, R. Clérac, J. M. Koomen, D. H. Russell and K. R. Dunbar, *J. Am. Chem. Soc.*, 2001, **123**, 773; (*e*) G. Yang and R. G. Raptis, *Dalton Trans.*, 2002, 3936; (*f*) E. Ruiz, J. Cano, S. Alvarez, A. Caneschi and D. Gatteschi, *J. Am. Chem. Soc.*, 2003, **125**, 6791; (*g*) C. Cañada-Vilalta, T. A. O'Brien, M. Pink, E. R. Davidson and G. Christou, *Inorg. Chem.*, 2003, **42**, 7819; (*h*) S. Lin, S.-X. Liu, Z. Chen, B.-Z. Lin and S. Gao, *Inorg. Chem.*, 2004, **43**, 2222; (*i*) E. M. Rumberger, L. N. Zakharov, A. L. Rheingold and D. N. Hendrickson, *Inorg. Chem.*, 2004, **43**, 6531; (*j*) G. Mezei, P. Baran and R. G. Raptis, *Angew. Chem., Int. Ed.*, 2004, **43**, 574; (*k*) D. Foguet-Albiol, K. A. Abboud and G. Christou, *Chem. Commun.*, 2005, 4282; (*l*) R. P. John, K. Lee, B. J. Kim, B. J. Suh, H. Rhee and M. S. Lah, *Inorg. Chem.*, 2005, **44**, 7109; (*m*) C. S. Campos-Fernández, B. L. Schottel, H. T. Chifotides, J. K. Bera, J. Bacsa, J. M. Koomen, D. H. Russell and K. R. Dunbar, *J. Am. Chem. Soc.*, 2005, **127**, 12909; (*n*) D. M. Low, G. Rajaraman, M. Helliwell, G. Timco, J. van Slageren, R. Sessoli, S. T. Ochsenbein, R. Bircher, C. Dobe, O. Waldmann, H.-U. Güdel, M. A. Adams, E. Ruiz, S. Alvarez and E. J. L. McInnes, *Chem.–Eur. J.*, 2006, **12**, 1385; (*o*) Z.-H. Ni, L.-F. Zhang, V. Tangoulis, W. Wernsdorfer, A.-L. Cui, O. Sato and H.-Z. Kou, *Inorg. Chem.*, 2007, **46**, 6029; (*p*) L. P. Engelhardt, C. A. Muryn, R. G. Pritchard, G. A. Timco, F. Tuna and R. E. P. Winpenny, *Angew. Chem., Int. Ed.*, 2008, **47**, 924.

6 Pecoraro's metallacrown: (*a*) J. T. Grant, J. Jankolovitz and V. L. Pecoraro, *Inorg. Chem.*, 2012, **51**, 8034; (*b*) J. Jankolovits, C. M. Andolina, J. W. Kampf, K. N. Raymond and V. L. Pecoraro, *Angew. Chem., Int. Ed.*, 2011, **50**, 9660; (*c*) C. Zaleski, S. Tricard, E. C. Depperman, W. Wernsdorfer, T. Mallah, M. L. Kirk and V. L. Pecoraro, *Inorg. Chem.*, 2011, **50**, 11348; (*d*) C. Zaleski, C. S. Lim, A. C. van Noord, J. W. Kampf and V. L. Pecoraro, *Inorg. Chem.*, 2011, **50**, 7707; (*e*) C. S. Lim, J. Jankolovits, P. Zhao, J. W. Kampf and V. L. Pecoraro, *Inorg. Chem.*, 2011, **50**, 4832; (*f*) T. T. Boron, J. W. Kampf and V. L. Pecoraro, *Inorg. Chem.*, 2010, **49**, 9104; (*g*) M. Tegoni, M. Furlotti, M. Tropiano, C. S. Lim and V. L. Pecoraro, *Inorg. Chem.*, 2010, **49**, 5190; (*h*) J. Jankolovits, J. W. Kampf and V. L. Pecoraro, *Chem.–Eur. J.*, 2010, **16**, 6786; (*i*) C. S. Lim, J. Jankolovits, J. W. Kampf and V. L. Pecoraro, *Chem.–Asian J.*, 2010, **5**, 46; (*j*) P. D. Ellis, A. S. Lipton, J. A. Sears, P. Yang, M. Dupuis, T. T. Boron, V. L. Pecoraro, T. Stich and R. D. Britt, *J. Am. Chem. Soc.*, 2010, **132**, 16727; (*k*) J. Gätjens, J. W. Kampf, P. Thuéry and V. L. Pecoraro, *Dalton Trans.*, 2009, 51–62; (*l*) C. S. Lim, J. W. Kampf and V. L. Pecoraro, *Inorg. Chem.*, 2009, **48**, 5224; (*m*) G. Micera, V. L. Pecoraro and E. Garribba, *Inorg. Chem.*, 2009, **48**, 5790; (*n*) L. Tabares, J. Gätjens, C. Hureau, M. R. Burrell, L. Bowater, V. L. Pecoraro, S. Bornemann and S. Un, *J. Phys. Chem.*, 2009, **113**, 9016.

7 Saalfrank's ring: (*a*) R. W. Saalfrank, N. Low, F. Hampel and H.-D. Stachel, *Angew. Chem., Int. Ed.*, 1996, **35**, 2209; (*b*) R. W. Saalfrank, I. Bernt, E. Uller and F. Hampel, *Angew. Chem., Int. Ed.*, 1997, **36**, 2482; (*c*) R. W. Saalfrank, T. Nakajima, N. Mooren, A. Scheurer, H. Maid, F. Hampel, C. Trieflinger and J. Daub, *Eur. J. Inorg. Chem.*, 2005, 1149.

8 Peng's wire: (*a*) S.-J. Shieh, C.-C. Chou, G.-H. Lee, C.-C. Wang and S.-M. Peng, *Angew. Chem., Int. Ed.*, 1997, **36**, 56; (*b*) I.-W. P. Chen, M.-D. Fu, W.-H. Tseng, J.-Y. Yu, S.-H. Wu, C.-J. Ku, C.-h. Chen and S.-M. Peng, *Angew. Chem., Int. Ed.*, 2006, **45**, 5814; (*c*) I. P.-C. Liu, M. Bénard, H. Hasanov, I.-W. P. Chen, W.-H. Tseng, M.-D. Fu, M.-M. Rohmer, C.-h. Chen, G.-H. Lee and S.-M. Peng, *Chem.–Eur. J.*, 2007, **13**, 8667; (*d*) C.-H. Chien, J.-C. Chang, C.-Y. Yeh, G.-H. Lee, J.-M. Fang and S.-M. Peng, *Dalton Trans.*, 2006, 2106; (*e*) C. Yin, G.-C. Huang, C.-K. Kuo, M.-D. Fu, H.-C. Lu, J.-H. Ke, K.-N. Shih, Y.-L. Huang, G.-H. Lee, C.-Y. Yeh, C.-h. Chen and S.-M. Peng, *J. Am. Chem. Soc.*, 2008, **130**, 10090.

9 Lehn's helicate: (*a*) R. Krämer, J.-M. Lehn, A. De Cian and J. Fischer, *Angew. Chem., Int. Ed.*, 1993, **32**, 703; (*b*) K. T. Potts, C. P. Horwitz, A. Fessak, K. M. Keshavarz, K. E. Nash and P. J. Toscano, *J. Am. Chem. Soc.*, 1993, **115**, 10444; (*c*) J.-M. Lehn and A. Rigault, *Angew. Chem., Int. Ed.*, 1988, **27**, 1095; (*d*) A.-M. Stadler, N. Kyritsakas, G. Vaughan and J.-M. Lehn, *Chem.–Eur. J.*, 2007, **13**, 59.

10 Helicate: (*a*) R. Ishikawa, M. Nakano, A. Fuyuhiro, T. Takeuchi, S. Kimura, T. Kashiwagi, M. Hagiwara, K. Kindo, S. Kaizaki and S. Kawata, *Chem.–Eur. J.*, 2010, **16**, 11139; (*b*) K. Yoneda, K. Adachi, K. Nishio, M. Yamasaki, A. Fuyuhiro, M. Katada, S. Kaizaki and S. Kawata, *Angew. Chem., Int. Ed.*, 2003, **45**, 5459; (*c*) S. Romain, J. Rich, C. Sens, T. Stoll, J. Benet-Buchholz, A. Llobet, M. Rodriguez, I. Romero, R. Clérac, C. Mathonière, C. Duboc, A. Deronzier and M.-N. Collomb, *Inorg. Chem.*, 2011, **50**, 8427.

11 Cage: (*a*) M. Fujita, M. Tominaga, A. Hori and B. Therrien, *Acc. Chem. Res.*, 2005, **38**, 369; (*b*) D. Fiedler, D. H. Leung, R. G. Bergman and K. N. Raymond, *Acc. Chem. Res.*, 2005, **38**, 349; (*c*) S. R. Seidel and P. J. Stang, *Acc. Chem. Res.*, 2002, **35**, 972; (*d*) J. J. Perry, J. A. Perman and M. J. Zaworotko, *Chem. Soc. Rev.*, 2009, **38**, 1400; (*e*) M. D. Pluth, R. G. Bergman and K. N. Raymond, *Acc. Chem. Res.*, 2009, **42**, 1650; (*f*) M. D. Ward, *Chem. Commun.*, 2009, 4487.

12 SMMs: (*a*) R. Sessoli, D. Gatteschi, A. Caneshi and M. A. Novak, *Nature*, 1993, **365**, 141; (*b*) G. Christou, D. Gatteschi, D. N. Hendrickson and R. Sessoli, *MRS Bull.*, 2000, **25**, 66; (*c*) D. Gatteschi and R. Sessoli, *Angew. Chem., Int. Ed.*, 2003, **42**, 268; (*d*) G. Aromi and E. K. Brechin, *Struct. Bonding*, 2006, **122**, 1.

13 ETCST review: (*a*) G. N. Newton, M. Nihei and H. Oshio, *Eur. J. Inorg. Chem.*, 2011, 3031; (*b*) A. Bleuzen, V. Marvaud, C. Mathonière, B. Sieklucka and M. Verdaguer, *Inorg. Chem.*, 2009, **48**, 3453.

14 Multiredox complexes: (*a*) M. Ruben, E. Breuning, J.-P. Gisselbrecht and J.-M. Lehn, *Angew. Chem., Int. Ed.*, 2000, **39**, 4139; (*b*) M. Venturi, A. Credi and V. Balzani, *Coord. Chem. Rev.*, 1999, **185–186**, 233; (*c*) M. Abe, *Bull. Jpn. Soc. Coord. Chem.*, 2011, **58**, 20.

15 Polynuclear complexes with multidentate ligands: (*a*) R. Chakrabarty, P. S. Mukherjee and P. J. Stang, *Chem. Rev.*, 2011, **111**, 6810; (*b*) P. A. Vigato, V. Peruzzo and S. Tamburini, *Coord. Chem. Rev.*, 2012, **256**, 953.

16 S. Koizumi, M. Nihei, T. Shiga, M. Nakano, H. Nojiri, R. Bircher, O. Waldmann, H. U. Güdel and H. Oshio, *Chem.–Eur. J.*, 2007, **13**, 8445.

17 S. Yamashita, T. Shiga, M. Kurashina, M. Nihei, H. Nojiri, H. Sawa, T. Kakiuchi and H. Oshio, *Inorg. Chem.*, 2007, **46**, 3810.

18 (*a*) M. Nihei, Y. Sekine, N. Suganami, K. Nakazawa, A. Nakao, H. Nakao, Y. Murakami and H. Oshio, *J. Am. Chem. Soc.*, 2011, **133**, 3592; (*b*) M. Nihei, Y. Sekine, N. Suganami and H. Oshio, *Chem. Lett.*, 2010, 978.

19 (*a*) T. Shiga, G. N. Newton, J. S. Mathieson, T. Tetsuka, M. Nihei, L. Cronin and H. Oshio, *Dalton Trans.*, 2010, **39**, 4730; (*b*) T. Shiga, F. Iijima, T. Tetsuka, G. N. Newton and H. Oshio, *Macromol. Symp.*, 2012, **317–318**, 286.

20 T. Shiga, T. Matsumoto, M. Noguchi, T. Onuki, N. Hoshino, G. N. Newton, M. Nakano and H. Oshio, *Chem.–Asian J.*, 2009, **4**, 1660.

21 G. N. Newton, T. Onuki, T. Shiga, M. Noguchi, T. Matsumoto, J. S. Mathieson, M. Nihei, L. Cronin and H. Oshio, *Angew. Chem., Int. Ed.*, 2011, **50**, 4844.

22 Triazole bridged [Fe$_5$] cluster, T. Shiga, M. Noguchi, G. N. Newton and H. Oshio, unpublished result.

23 J. J. Borrás-Almenar, J. M. Clemente-Juan, E. Coronado and B. S. Tsukerblat, *J. Comput. Chem.*, 2001, **22**, 985.

24 BVS for **1**: Fe1, 2.611 for Fe^{II}, **3.043** for Fe^{III}; Fe2, 2.596 for Fe^{II}, **3.026** for Fe^{III}; Fe3, **1.873** for Fe^{II}, 2.121 for Fe^{III}.

25 X. Bao, J.-D. Leng, Z.-S. Meng, Z. Lin, M.-L. Tong, M. Nihei and H. Oshio, *Chem.–Eur. J.*, 2010, **16**, 6169.

26 BVS for **2**: (*a*) O1, 1.189, O2, 1.165, O3, 1.071, O4, 1.069, O5, 1.072, O6, 1.048, O7, 0.763, O8, 0.757, O9, 0.780, O10, 0.698, O11, 0.679, O12, 0.685 (all values suggest hydroxide ions); (*b*) Fe1, 2.566 for Fe^{II}, **2.97** for Fe^{III}; Fe2, **2.116** for Fe^{II}, 2.442 for Fe^{III}; Fe3, **2.053** for Fe^{II}, 2.37 for Fe^{III}; Fe4, 3.571 for Fe^{II}, **4.257** for Fe^{III}; Fe5, 3.278 for Fe^{II}, **3.907** for Fe^{III}; Fe6, **2.001** for Fe^{II}, 2.266 for Fe^{III}; Fe7, **2.099** for Fe^{II}, 2.377 for Fe^{III} (calculated using values from W. Liu and H. H. Thorp, *Inorg. Chem.*, 1993, **32**, 4102.

27 BVS for **3**: Fe1, 2.343 for Fe^{II}, **2.734** for Fe^{III}; Fe2, 2.296 for Fe^{II}, **2.737** for Fe^{III}; Fe3, 2.489 for Fe^{II}, **2.887** for Fe^{III}; Fe4, 2.493 for Fe^{II}, **2.887** for Fe^{III}.

28 G. W. Powell, H. N. Lancashire, E. K. Brechin, D. Collison, S. L. Heath, T. Mallah and W. Wernsdorfer, *Angew. Chem., Int. Ed.*, 2004, **43**, 5772.

29 [Fe$_{19}$] cluster: D. M. Low, L. F. Jones, A. Bell, E. K. Brechin, T. Mallah, E. Rivière, S. J. Teat and E. J. L. McInnes, *Angew. Chem., Int. Ed.*, 2003, **42**, 3781.

30 Ferritin: B. L. d'Estaintot, P. Santambrogio, T. Granier, B. Gallois, J. M. Chevalier, G. Precigoux, S. Levi and P. Arosio, *J. Mol. Biol.*, 2004, **340**, 277.

31 (*a*) D. Piñero, P. Baran, R. Boca, R. Herchel, M. Klein, R. G. Raptis, F. Renz and Y. Sanakis, *Inorg. Chem.*, 2007, **46**, 10981; (*b*) B. Burger, S. Demeshko, E. Bill, S. Dechert and F. Meyer, *Angew. Chem., Int. Ed.*, 2012, **51**, 10045.

32 K. Nakano, N. Suemura, S. Kawata, A. Fuyuhiro, T. Yagi, S. Nasu, S. Morimoto and S. Kaizaki, *Dalton Trans.*, 2004, 982.

33 E. Spodine, A. M. Atria, J. Valenzuela, J. Jalocha, J. Manzur, A. M. García, M. T. Garland, O. Peñac and J.-Y. Saillard, *J. Chem. Soc., Dalton Trans.*, 1999, 3029.

34 Redox potential of [Fe(bpy)$_3$]: N. G. Connelly and W. E. Geiger, *Chem. Rev.*, 1996, **98**, 877.

35 (*a*) A. L. Spek, *J. Appl. Crystallogr.*, 2003, **36**, 7; (*b*) P. v. d. Sluis and A. L. Spek, SQUEEZE, *Acta Crystallogr., Sect. A: Found. Crystallogr.*, 1990, **46**, 194.